

## Unambiguous Evidence for Efficient Chemical Catalysis of Adenosine Ester Aminolysis by Its 2'/3'-OH

Stanislav G. Bayryamov, Miroslav A. Rangelov, Aneta P. Mladjova, Vihra Yomtova, and Dimitar D. Petkov\*

Laboratory of BioCatalysis, Institute of Organic Chemistry, Bulgarian Academy of Sciences, Sofia 1113, Bulgaria

Received November 24, 2006; E-mail: dd5kov@orgchm.bas.bg

Peptide bond formation by alkyl ester aminolysis is a very slow reaction and requires a proton transfer catalyst in order to proceed at a measurable rate.<sup>1</sup> As a three-molecular reaction, it involves a large entropy loss which accounts for the extremely slow rates. During protein biosynthesis,<sup>2</sup> this entropy problem is solved by binding of the two substrates and the catalyst in a proper configuration, which transforms the slow three-molecular reaction into a very fast intracomplex one. This could mean that the ribosome provides favorable configurational entropy for efficient catalysis by the proton transfer catalyst—the 3'-terminal adenosine 2'-OH of the peptidyl tRNA. The verification of this hypothesis requires studies of both the ribosome and model systems. The current mechanistic proposals are dominated by the idea of the ribosome being a template for entropic activation only without providing acid–base catalytic groups.<sup>3</sup> Here, we report on computational and experimental studies of intramolecular aminolysis reactions, catalyzed by a vicinal OH group. They were designed as model reactions (Chart 1) of the ribosome intracomplex aminolysis in order to find support for the crucial role of the 3'-terminal adenosine 2'-OH of the peptidyl tRNA as acid–base catalyst in the ribosome peptidyl transfer.

Quite recently<sup>4</sup> we reported a computational study of the mechanism and energetics of the simplest model of the reaction naturally catalyzed by the ribosome—the ammonolysis of 1-*O*-formyl 1,2-ethanediol **1** (Chart 1). The favored pathway predicted by calculations is a stepwise addition/elimination in which addition and elimination are coupled with *syn*-2-OH-assisted proton shuttling to maintain the neutrality of the tetrahedral intermediate formed. The model substrate **1** is designed to possess enantiotopic rather than diastereotopic re and si faces of the ester carbonyl and the amine attack produces R and S transition states/tetrahedral intermediates with the same energy and mirror-image structures. To model the intramolecularity of the ribosome aminolysis reaction, we now study the aminolysis of 1-*O*- $\delta$ -aminovaleryl 1,2-ethanediol **2**, in which the NH<sub>2</sub> group is an integral part of the substrate and attacks the pro-S face of the ester carbonyl (Chart 1) as does probably  $\alpha$ -NH<sub>2</sub> of the aminoacyl tRNA during the ribosome reaction.<sup>3d</sup> The calculations were performed at the B3LYP level with the 6-31G(d,p) basis set.<sup>4</sup>

Our reference reaction is the ammonolysis of 1-*O*-formyl 1,2-ethanediol with an anti-oriented 2-OH **1a** (Chart 1), in which neither 2-OH nor  $\delta$ -NH<sub>2</sub> can exert a proximity effect. The calculated reduction of the activation Gibbs free energy of the reference reaction  $\Delta\Delta G^*$ , caused by the proximity effects in the addition and elimination transition states **TS1** and **TS2** of the stepwise mechanism, is shown in Table 1. The design of the substrates allows us to calculate the individual contribution to  $\Delta\Delta G^*$  of (a) the intramolecular attack of *syn*- $\delta$ -NH<sub>2</sub> **2a**, (b) the intramolecular catalysis by *syn*-2-OH **1b**, and (c) the combined action of *syn*-2-OH and *syn*- $\delta$ -NH<sub>2</sub> **2b** (Chart 1).

Chart 1

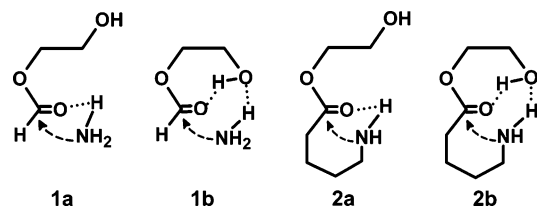


**Table 1.** Calculated Reduction of  $\Delta G^*$ ,  $\Delta H^*$ , and  $T\Delta S^*$  of the Reference Aminolysis Reaction **1a** by an Intramolecular Pro-S Attack of *syn*- $\delta$ -NH<sub>2</sub> (**2a**), an Intramolecular Participation of *syn*-2-OH (**1b**), and Their Combined Effect (**2b**), Associated with the First, Second, and Rate-Determining Transition States **TS1**, **TS2**, and **RDTs**

|           | <b>TS1</b>         |                    |                     | <b>TS2</b>         |                    |                     | <b>RDTs</b>        |                    |                     |
|-----------|--------------------|--------------------|---------------------|--------------------|--------------------|---------------------|--------------------|--------------------|---------------------|
|           | $\Delta\Delta G^*$ | $\Delta\Delta H^*$ | $T\Delta\Delta S^*$ | $\Delta\Delta G^*$ | $\Delta\Delta H^*$ | $T\Delta\Delta S^*$ | $\Delta\Delta G^*$ | $\Delta\Delta H^*$ | $T\Delta\Delta S^*$ |
| <b>1a</b> | 0                  | 0                  | 0                   | 0                  | 0                  | 0                   | 0                  | 0                  | 0                   |
| <b>2a</b> | 6.5                | -1.0               | -7.5                | 11.0               | 3.3                | -7.7                | 6.5                | -1.0               | -7.5                |
| <b>1b</b> | 22.5               | 26.3               | 3.8                 | 8.1                | 10.2               | 2.1                 | 15.9               | 17.5               | 1.6                 |
| <b>2b</b> | 32.8               | 29.2               | -3.6                | 16.9               | 11.8               | -5.1                | 24.7               | 19.1               | -5.6                |

Characteristically, in the first transition state **TS1**, the reduction of  $\Delta\Delta G^*$  induced by *syn*-OH catalysis (22.5 kcal/mol for **1b**) is more than three times larger than the reduction caused by the intramolecularity of the  $\delta$ -NH<sub>2</sub> attack (6.5 kcal/mol for **2a**). The combined proximity effect of the two groups is synergistic (32.8 kcal/mol for **2b**). On the contrary, the proximity effect of *syn*- $\delta$ -NH<sub>2</sub> in the second transition state **TS2** is even higher than that of *syn*-2-OH, and their combined effect is almost additive (Table 1).

Thus, the calculated variations in  $\Delta\Delta G^*$  match the effect of the transition state proton transfer geometry,<sup>4</sup> suggesting a domination of *syn*-2-OH proton shuttling catalysis in the acceleration of the aminolysis. This conclusion is supported by the variation of the calculated enthalpic and entropic contributions  $\Delta\Delta H^*$  and  $T\Delta\Delta S^*$  (Table 1). Actually, the entropic contribution in both the first and second transition states of **2a** aminolysis exceeds the enthalpic contribution due to the unfavorable direct proton transfer in the absence of the *syn*-OH assistance.<sup>4</sup> On the contrary, the enthalpic contribution to the reduction of the free energy of the two transition states in **1b** and **2b** is 2–6 times larger than the entropic contribution (Table 1) due to the effective *syn*-2-OH-assisted proton shuttling.<sup>4</sup> Therefore, the driving force for the acceleration of the model aminolysis reaction is the proton shuttling catalysis by *syn*-2-OH.

The experimental determination of  $\Delta H^*$  and  $\Delta S^*$  requires dissection of  $\Delta G^*$  into enthalpy and entropy contributions. However, this cannot be done for  $\Delta G^*$  determined in aqueous solutions because of the enthalpy–entropy compensation in water:<sup>5</sup> the measured values contain contributions from  $\Delta H_{\text{sol}}$  and  $\Delta S_{\text{sol}}$  that cancel out in  $\Delta G^*$  but may obscure measured  $\Delta H^*$  and  $\Delta S^*$ . On

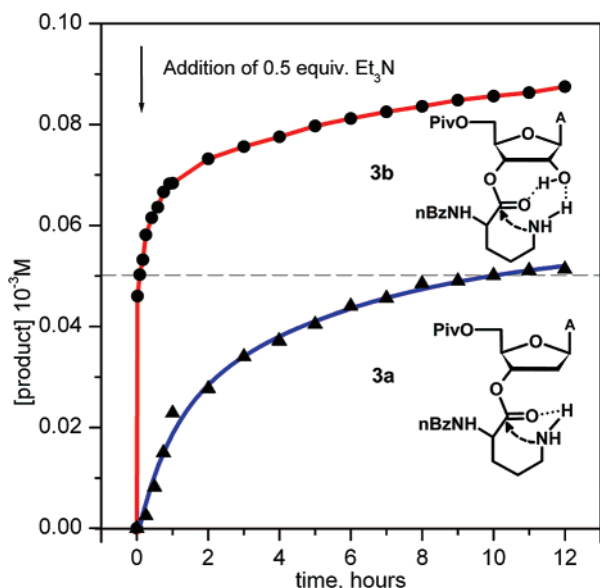


**Figure 1.** Time course of the intramolecular aminolysis (lactamization) in acetonitrile at 25 °C of 0.1 mmol trifluoroacetate of 2'/3'-O-( $\alpha$ -N-p-nitrobenzoyl ornithinyl) 5'-O-pivaloyl adenosine **3b** and deoxyadenosine **3a** to  $\alpha$ -N-p-nitrobenzoyl cyclic ornithine after addition of 1/2 equiv of  $\text{Et}_3\text{N}$ .

the basis of such experimental data, the ribosome has been considered as an entropy trap.<sup>3a</sup> On the other hand, the computer simulation approaches predict a larger contribution of the solvation entropy  $\Delta S_{\text{sol}}$  than of the solute configurational entropy  $\Delta S_{\text{prox}}$  considered here. The authors, however, do not mention the ratio of the corresponding enthalpic contributions,  $\Delta H_{\text{sol}}$  and  $\Delta H_{\text{prox}}$ .<sup>6b</sup>

The acceleration of the overall aminolysis reaction is associated with the decrease in the activation energy of the rate-limiting transition state  $\Delta\Delta G^*$  (Table 1). The difference between the values for intramolecular aminolysis of 1-O- $\delta$ -aminovaleryl 1,2-ethanediol with (**2b**) and without (**2a**) participation of 2-OH is 18.2 kcal/mol, which corresponds to a more than billion-fold ( $2.2 \times 10^{13}$ ) rate acceleration. In order to check this prediction of the theory, we prepared 2'/3'-O-( $\alpha$ -N-p-nitrobenzoyl-L-ornithinyl) 5'-O-pivaloyl adenosine **3b** and its 2'-deoxy analogue **3a** and studied the time course of their intramolecular aminolysis to the corresponding  $\delta$ -lactam ( $\alpha$ -N-p-nitrobenzoyl cyclic L-ornithine) in the polar organic solvent acetonitrile. After the addition of 1/2 equiv of  $\text{Et}_3\text{N}$  to 0.1 mmol of trifluoroacetate of the adenosine ester **3b**, an initial "burst" formation of ca. 0.05 mmol of cyclic L-ornithine, followed by a much slower release, was observed (Figure 1). The biphasic nature of the time course suggests the occurrence of two consecutive reactions, the first one being that of the free base  $\delta$ -NH<sub>2</sub> and the second that of its trifluoroacetate salt. Under the same conditions, however, only slow aminolysis by  $\delta$ -NH<sub>2</sub> is registered in the case of the deoxy analogue **3a**. The estimated minimal rate constant ratio of the aminolysis of adenosine and deoxyadenosine ester is ca. 3600.<sup>7</sup> Therefore, while the lactamization of the adenosine ester **3b** is instantaneous (the reaction being over during the mixing of the reagents and its quenching in the analytical sample (10 s)), that of the deoxyadenosine ester **3a** is not over until 10 h (Figure 1). Since the only difference in the substrates is the presence or not of the 2'-OH, the observed dramatic acceleration in the case of the adenosine ester can only be attributed to the catalysis by the 2'-

OH group. To the best of our knowledge, this is the first unequivocal experimental evidence for efficient chemical catalysis of adenosine ester aminolysis by its 2'-OH group in a nonribosomal reaction.

The dramatic difference in the aminolysis rate of the adenosine and deoxyadenosine esters approaches the large difference in reactivity of peptidyl tRNA and its 2'-deoxy mutant in the ribosome fragment reaction.<sup>8</sup> The parallel change in the reactivity of the model and ribosome reaction, however, do not necessarily imply that the ribosome provides a microenvironment resembling that of a polar aprotic solvent. However, as established by molecular dynamic simulation studies,<sup>6</sup> enzymes and particularly the ribosome use preorganized polar electrostatic environment to catalyze the corresponding reactions. The observed time course of our bioorganic model reactions indicates that the non-hydrogen-bonding polar organic solvent acetonitrile is the simplest model of the ribosome polar electrostatic environment of the rate-limiting transition state.

After the formation of the ribosome–substrate complex, each of the ribosome substrates becomes an integral part of the ribosome and the participation of substrate acid–base groups in the catalytic process is possible. This reminds us of the formation of a holoenzyme from an apoenzyme and coenzyme, the latter being the ribosome and peptidyl tRNA, respectively. Recent studies of ribosome–substrate crystal structures<sup>3d</sup> reveal that the 2'-OH of the peptidyl tRNA 3'-terminal adenosine hydrogen bonds to aminoacyl tRNA  $\alpha$ -NH<sub>2</sub> and is the only functional group positioned to act as a general base. The deleterious effect of its removal on ribosome catalysis<sup>9</sup> and the dramatic change in the aminolysis rate after deletion of the adenosine 2'-OH observed here strongly support its significant catalytic role in substrate-assisted ribosome catalysis.

**Acknowledgment.** Supported by grants from the National research Fund of Bulgaria (grants X-1001 and X-1517). We thank I.G. Pojarlieff for helpful and stimulating discussions.

**Supporting Information Available:** Computational details and data, synthesis and characterization of the substrates, and description of the kinetic experiments. This material is available free of charge via the Internet at <http://pubs.acs.org>.

## References

- (1) Satterthwait, A. C.; Jencks, W. P. *J. Am. Chem. Soc.* **1974**, *96*, 7018–7031.
- (2) Wilson, D. N.; Nierhaus, K. N. *Angew. Chem., Int. Ed.* **2003**, *42*, 3464–3486.
- (3) (a) Sievers, A.; Beringer, M.; Rodnina, M. V.; Wolfenden, R. *Proc. Natl. Acad. Sci. U.S.A.* **2004**, *117*, 7897–7901. (b) Youngman, E. M.; Brunelle, J. L.; Kochniak, A. B.; Green, R. *Cell* **2004**, *117*, 589–599. (c) Chagalov, M. M.; Ivanova, G. D.; Rangelov, M. A.; Acharia, P.; Acharia, S.; Minakawa, N.; Foldesi, A.; Stoineva, I. B.; Yomtova, V. M.; Roussev, C. D.; Matsuda, A.; Chattopadhyaya, J.; Petkov, D. D. *ChemBioChem* **2005**, *6*, 972–977. (d) Martin Schmeiling, T.; Huang, K. S.; Kitchen, D. E.; Strobel, S. A.; Steitz, T. A. *Mol. Cell* **2005**, *20*, 437–448. (e) Rodnina, M.; Beringer, M.; Wintermeyer, W. *Quart. Rev. Biophys.* **2006**, *39*, 203–225. (f) Chagalov, M. M.; Petkov, D. D. *Tetrahedron Lett.* **2007**, *48*, 2381–2384.
- (4) Rangelov, M. A.; Vayssilov, G.; Yomtova, V. M.; Petkov, D. D. *J. Am. Chem. Soc.* **2006**, *128*, 4964–4965 and details are found in the Supporting Information.
- (5) Dunitz, J. D. *Chem. Biol.* **1995**, *2*, 709–712.
- (6) (a) Trobo, S.; Aqvist, J. *Proc. Natl. Acad. Sci. U.S.A.* **2005**, *102*, 12395–12400. (b) Sharma, P. K.; Xiang, Y.; Kato, M.; Warshel, A. *Biochemistry* **2005**, *44*, 11307–11314. (c) Warshel, A. *J. Biol. Chem.* **1995**, *273*, 27035–27038.
- (7) The estimation is found under Supporting Information.
- (8) Chinali, G.; Sprinzl, M.; Parmeggiani, A.; Cramer, F. *Biochemistry* **1974**, *13*, 3001–3010.
- (9) (a) Hecht, S. *Tetrahedron* **1977**, *33*, 1671–1696. (b) Weinger, J. S.; Parnell, K. M.; Dorner, S.; Green, R.; Strobel, S. A. *Nat. Struct. Mol. Biol.* **2004**, *11*, 1101–1106.

JA068447G